Evaluation of modified four-component scattering power decomposition method over highly rugged glaciated terrain

Gulab Singh[1], Y. Yamaguchi[1], S-E. Park[1] and Ram Avatar[2]
[1]Graduate School of Science and Technology, Niigata University, Ikarashi 2-8050, Niigata, Japan- 950-2181
[2]Department of Civil Engineering, The University of Tokyo, Tokyo, Japan-153-8505

Abstract: In recent years, there is increased the utilization of fully polarimetric synthetic aperture radar (POLSAR) data to study glaciated terrain features for glaciological and climate change modeling. This paper concern more accurate results and appropriate analysis of POLSAR data over highly rugged glaciated area in Himalayan region. For this purpose, the modified Yamaguchi four-component scattering power decomposition method with a rotation concept of 3 x 3 coherency matrix [*T*] about line of sight is evaluated. It has been found that the modified Yamaguchi four-component scattering power decomposition (4-CSPD) method significantly improved the decomposition results as compared to original 4-CSPD by the minimizing the cross-polarized (*HV*) components. This modified 4-CSPD leads the enhancement in the double bounce scattering and surface scattering components and also avoids the over-estimation problem in volume scattering component as compared to original 4-CSPD from the sloped terrain. The significant reductions of the negative power occurrence in the surface scattering (3.9%) and the double bounce scattering (19.7%) components have also been noticed as compared to original 4-CSPD method over the glaciated area in the part of Indian Himalaya.

Keywords: *Four component scattering power decomposition, PALSAR, Himalaya, glaciated terrain*.

1. Introduction

Detection of glaciated terrain features are important for hydrological and climate change modeling. Optical and near-infrared remote sensing techniques are very sensitive to cloud cover and different weather conditions, although they are promising for glaciated terrain mapping (Dozier 1989, Mohite *et. al.* 2007, Rott 1994). Microwave remote sensing using active sensing with Synthetic Aperture Radar

(SAR) has advantages such as cloud penetration, all-weather capability, and independence of sun illumination. SAR information add considerable robustness to identify the glaciated terrain (Singh and Venkataraman 2009) and potentially allows the retrieval of additional snow parameters connected to surface roughness and wetness, as well as internal snow structure and glacier movement (Shi and Dozier 1995, 2000, Partington 1998, Michel and Rignot 1999, Gray *et. al.*1998). With fully polarimetric capabilities of newer generation spaceborne SAR sensors are expected to lead to significant improvements in automated glaciated terrain feature identification based on polarimetric scattering decomposition theorem (Singh 2010). The main purpose of scattering decomposition methods is to decompose different scattering contributions in the polarimetric backscattering signature within the resolution cell. Polarimetric SAR data decompositions are also important to interpret or segment the glaciated terrain features and to develop the methodology for glacier parameters retrieval.

Several incoherent decomposition methods are published (Cloude and Pottier 1996, Yamaguchi *et. al*. 2006, Yajima *et. al.* 2008, Freeman and Durden 1998). Out of several incoherent decomposition methods, scattering power decomposition methods are attractive. These methods (Yamaguchi *et. al*. 2006, Yajima *et. al.* 2008, Freeman and Durden 1998) show straightforward implementation, the decomposed powers correspond to physical scattering mechanisms and output color-coded images are directly recognizable and easy to understand (Singh *et. al.* 2011b). Mountainous region topography has gentle to steep slope. This slope behaves like oriented surface from the direction of radar illumination, and oriented surface does not hold reflection symmetry condition where the Freeman and Durden three-component decomposition (Freeman and Durden 1998) method works, which causes the over estimation volume scattering in the Freeman and Durden three-component decomposition . It was expected, the over-estimated volume scattering power is reduced by the 4^{th} component in the four-component scattering power decomposition (4-CSPD) method (Yamaguchi *et. al*. 2006, Yajima *et. al.* 2008) under non-reflection condition (Singh *et. al.* 2011a). However, it has been found that the 4-CSPD

still has over estimation in the volume scattering power (Singh *et. al.* 2011b). Hence, this paper presents the results by using further modification of the 4-CSPD method with rotation of coherency matrix (Yamaguchi *et. al.* 2011, Singh *et. al.* 2010) on glaciated terrain features over the Satopanth glacier region in Himalaya. It is shown that improvement can be clearly seen in the highly rugged glacier region.

2. Study Area and Data Used

Satopanth and Bhagirath Kharak (BK) glaciers are the main glacier of the Alaknanda river catchment, Uttarakhand, India. The elevation ranges between 2000 m and 7000 m. The Alaknanda river, which is the main tributary of Ganga river, originates at the snout of the Satopanth glacier. The area locates between latitude 30^0 40' N and 30^0 50' N and longitude between 79^0 15' E and 79^0 28' E. Satopanth and Bhagirath Karak glaciated region more details are given in Singh *et. al.* (2011a).

In this study, the Phased Array type L-band Synthetic Aperture Radar (PALSAR) fully polarimetric, single look complex, level 1.1 data of May 12, 2007 with 21.5^0 incident angle and nominal pixel spacing (azimuth x range) 3.54 (m) x 9.36 (m) (www.eorc.jaxa.jp/ALOS/en/about/palsar.htm; www.palsar.ersdac.or.jp/e/index.html) has been used. The data set has been multi-looked 6 times in azimuth direction and 1 time in range direction for generating coherency matrix elements. After generating multi-looked coherency matrix, speckle noises were reduced by using refined Lee filter (Lee and Pottier 2009) with window size 5x5.

Snow cover area becomes wet in May (early summer) over Himalayan snow bound area with significant melting and the wet snowpack is not so transparent for L-band frequency (Singh *et. al.* 2011a). The co-polarization backscatters (HH and VV responses are nearly 10 times larger than the cross-polarization backscatter (HV or VH) responses (Singh 2010). Since the HV components

contribute to volume scattering and multiple scattering, the main polarimetric response from snowpack becomes surface scattering in the L-band (Singh *et. al.* 2011a, Abe et. al. 1990).

3. Method and Technique

3.1 4-CSPD Method

Scattering vector $\boldsymbol{k}$ can be defined in terms of scattering matrix **S** elements as

$$\boldsymbol{k} = \left(\frac{1}{\sqrt{2}}\right)[S_{HH} + S_{VV},\ S_{HH} - S_{VV}, 2S_{HV}]^{\dagger} \qquad (1)$$

where S_{HH}, S_{VV}, S_{HV} are elements of scattering matrix **S** assuming the reciprocal condition of $S_{HV} = S_{VH}$. The coherency matrix is given as

$$[\boldsymbol{T}] = \langle \boldsymbol{k}\boldsymbol{k}^{\dagger} \rangle = \begin{bmatrix} T_{11} & T_{12} & T_{13} \\ T_{21} & T_{22} & T_{23} \\ T_{31} & T_{32} & T_{33} \end{bmatrix} \qquad (2)$$

where † denotes complex conjugation and transposition, and ‹•› denotes ensemble average in an imaging window.

The four-component scattering power decomposition divides the measured coherency matrix into 4 sub-matrices representing physical scattering mechanisms (Yamaguchi *et. al*. 2006, Yajima *et. al.* 2008)

$$[T] = f_s[T_s] + f_d[T_d] + f_v[T_v] + f_c[T_c] \qquad (3)$$

where f_s, f_d, f_v and f_c are coefficients to be determined. [*Ts*], [T_d], [T_v] and [T_c] are expansion matrices corresponding to surface, double bounce, volume and helix scattering, respectively (Yamaguchi *et. al*. 2006, Yajima *et. al.* 2008).

3.2 Concept of [*T*] Rotation

Himalayan topography has gentle to very steep slope and this slope varies in azimuth as well as in range direction. In general, a lot of distortion occurs in backscattering from Himalayan region as compared to horizontal flat surface. It is pointed out (Lee et. al. 2000, 2002, Pottier 1998) that the polarization

orientation shift (or equivalently the cross-polarized component S_{HV}) is induced from the azimuthally sloped surface. In addition, the amount of the induced polarization orientation shift is a function of radar look angle and slope angle in range direction (Lee et. al. 2000, 2002, Pottier 1998). These effects in highly topographic surface can be reduced with help of polarization orientation compensation or minimization of the cross-polarized component. Since the T_{33} element of coherency matrix is the same as the cross-polarized component S_{HV} in scattering matrix, a method of rotation of coherency matrix to minimize its T_{33} element has been adopted. The idea of minimization of T_{33} element is also known as Deorientation (Lee and Pottier 2009, Xu and Jin 2005).

A general form of rotation of coherency matrix around the radar line of sight can be written as (Yamaguchi *et. al*. 2011)

$$[T'] = \begin{bmatrix} 1 & 0 & 0 \\ 0 & \cos 2\theta & \sin 2\theta \\ 0 & -\sin 2\theta & \cos 2\theta \end{bmatrix} [T] \begin{bmatrix} 1 & 0 & 0 \\ 0 & \cos 2\theta & -\sin 2\theta \\ 0 & \sin 2\theta & \cos 2\theta \end{bmatrix} \quad (4)$$

The rotated coherency matrix is denoted as $$[T'] = \begin{bmatrix} T_{11}(\theta) & T_{12}(\theta) & T_{13}(\theta) \\ T_{21}(\theta) & T_{22}(\theta) & T_{23}(\theta) \\ T_{31}(\theta) & T_{32}(\theta) & T_{33}(\theta) \end{bmatrix} \quad (5)$$

where

$$T_{33}(\theta) = T_{33}\cos^2 2\theta + T_{22}\sin^2 2\theta - \mathrm{Re}(T_{23})\sin 4\theta \quad (6)$$

It has been tried to minimize $T_{33}(\theta)$ term by rotation. The rotation angle can be found from

$$\frac{d}{d\theta} T_{33}(\theta) = 0 \quad (7)$$

$$\tan 4\theta = \frac{2\mathrm{Re}(T_{23})}{T_{22} - T_{33}} = \frac{4\mathrm{Re}\langle S_{HV}^{*} \ (S_{HH} - S_{vv})\rangle}{\langle |S_{HH} - S_{vv}|^2\rangle - 4\langle |S_{Hv}|^2\rangle} \quad (8)$$

This rotation angle is the same as the phase angle between two co-circular (left-left and right-right) polarization channels used to estimate azimuthal slope angle. Thus the minimization of $T_{33}(\theta)$ element yields the same angle. The angle in equation (8) will serve more accurate decomposition results over highly topographic mountainous area in comparison to the original coherency matrix method

(Yamaguchi *et. al*. 2006, Yajima *et. al.* 2008). The 4-CSPD method with rotation of coherency matrix is used for POLSAR data decomposition.

4. Results and Discussion

Firstly, the 4-CSPD method (Yamaguchi *et. al*. 2006, Yajima *et. al.* 2008) is applied to L-band PALSAR datasets over the Satopanth and BK glaciated region. Decomposed powers of surface scattering (Ps), double bounce scattering (Pd), volume scattering (Pv) and helix scattering (Pc) are shown in Fig. 1.

In order to examine the decomposed results of Fig. 1 quantitatively, the elevation map in this area is shown in Fig. 2(a), the slope angle map in Fig. 2(b), aspect (direction of slope) in Fig. 2(c). These topographic parameters are derived based on Advanced Spaceborne Thermal Emission and Reflection Radiometer-Global Digital Elevation Map (ASTER-GDEM) with 30 meter resolution (www.gdem.aster.ersdac.or.jp).

The angle derived by (8) is shown in Fig. 2(d). The rotation angle varies from -45^0 to $+45^0$. Noisy angle distribution has been seen in steep slope areas. The reason why we have made Fig. 2(d) is to examine a relation between the angle and negative power problem.

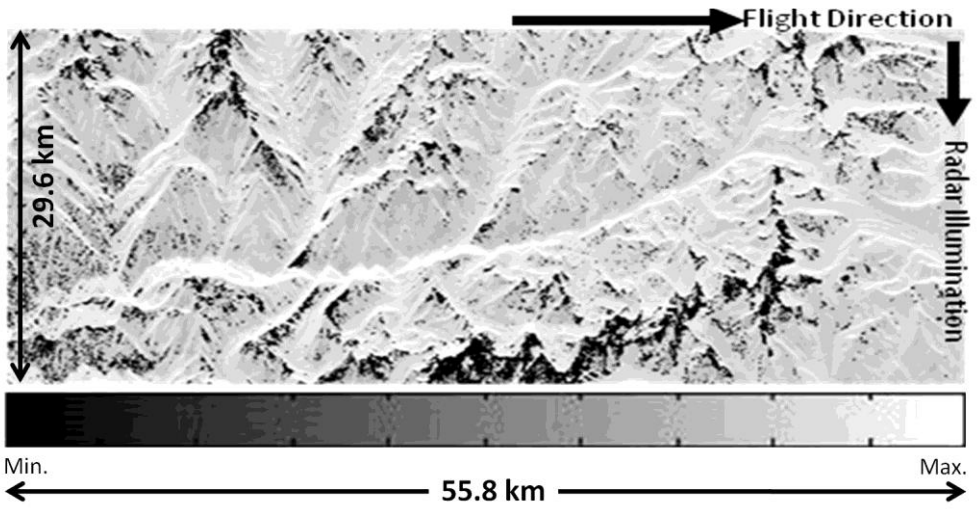

(a)

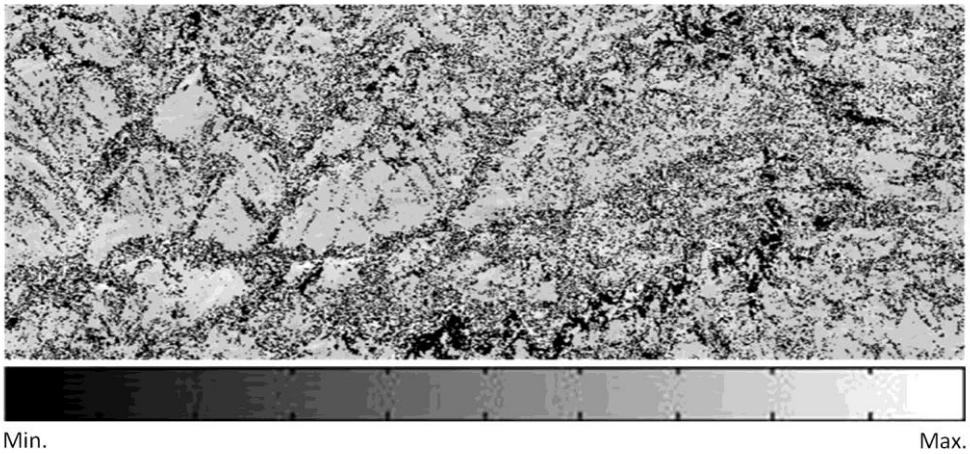

(b)

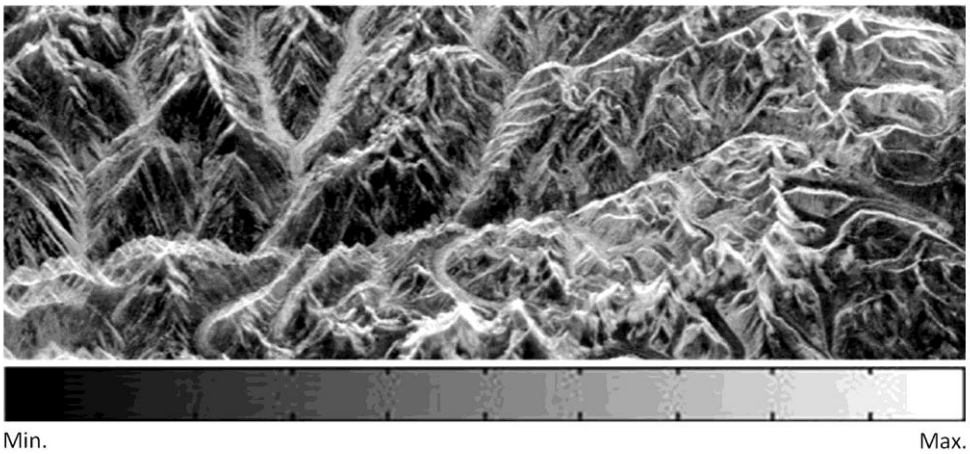

(c)

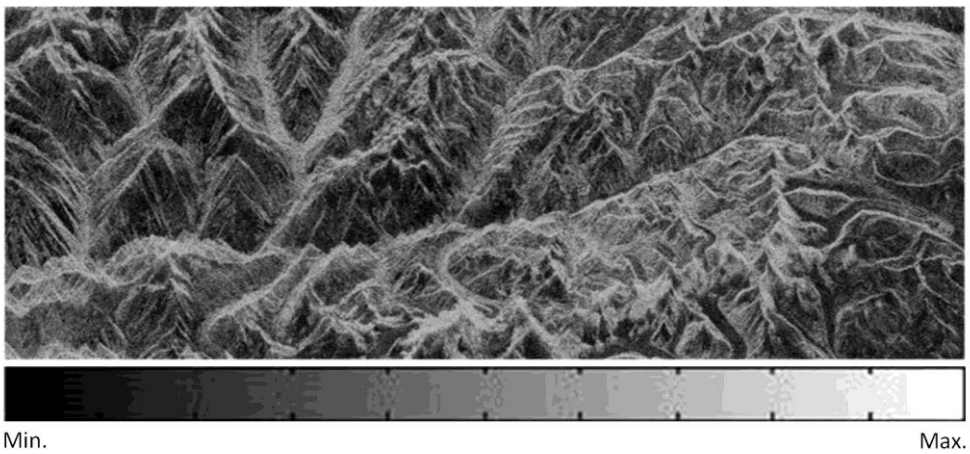

(d)

Fig. 1. Original 4-CSPD method decomposed powers (a) Ps, (b) Pd, (c) Pv, and (d) Pc. Black areas are 11.6% in Ps image (a) and are 29.5% in Pd image (b), which indicate the negative power occurred

pixels.

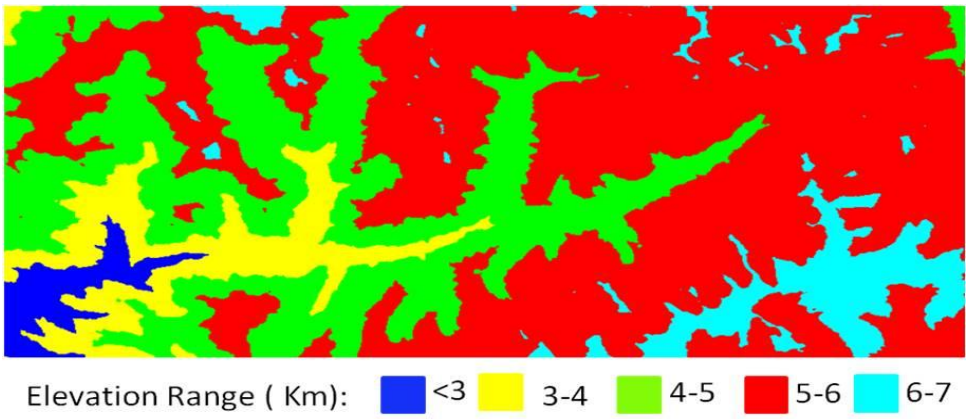
Elevation Range (Km):
<3
3-4
4-5
5-6
6-7

(a)

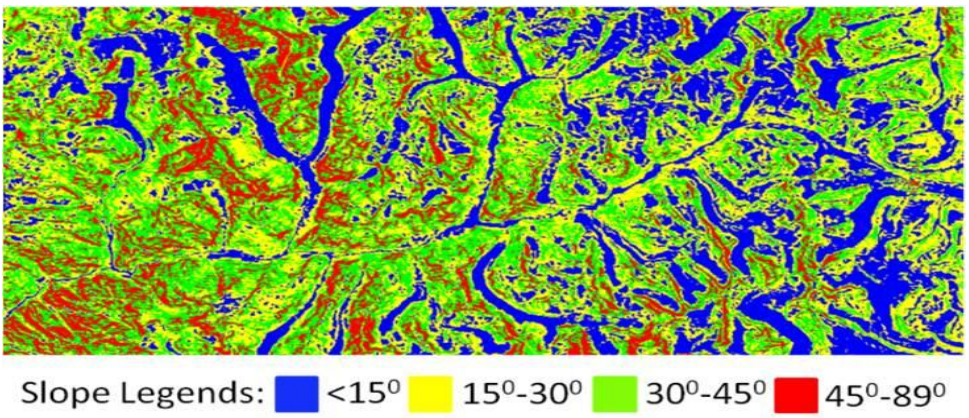
Slope Legends:
<15⁰
15⁰-30⁰
30⁰-45⁰
45⁰-89⁰

(b)

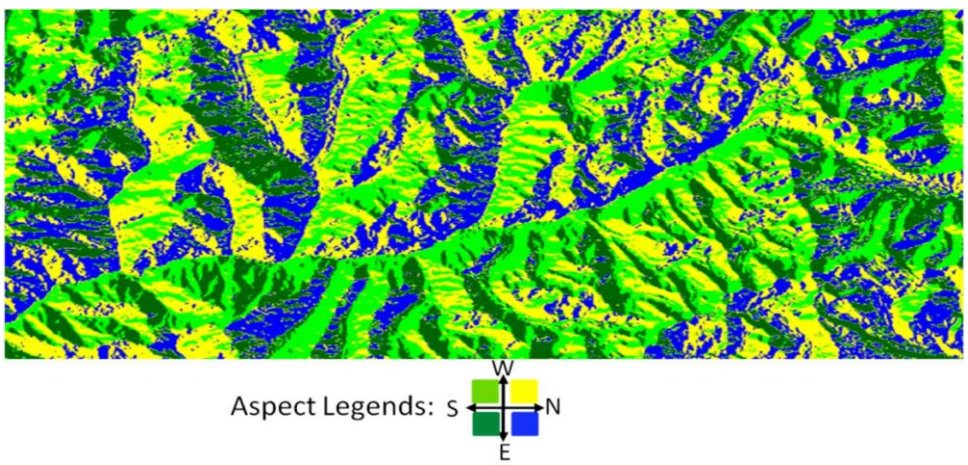
Aspect Legends:
W
S
N
E

(c)

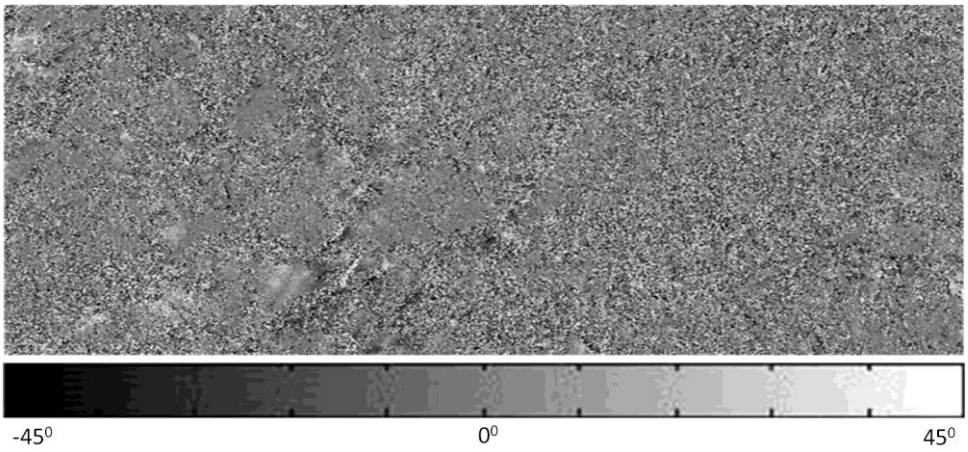

(d)

Fig. 2 (a) ASTER-GDEM (b) slope map (c) aspect (direction of slope) (d) Noisy rotation angle derived by equation (12) at steep slope areas

Percentages of pixels with negatives powers in surface scattering (Ps) and double bounce scattering component of original method are 11.6% and 29.5% respectively. It is seen in surface scattering (Ps) of Fig. 1(a) that the occurrences of negative power (black color) are less where slope is gentle and that the negative power occurrences are more at steep slope. Most of negative powers in Ps occurred in back slope area (N-E and S-E facing slope) i.e. in radar shadowing area.

On the other hand, in the double bounce power (Pd) image of Fig. 1(b), most of negative powers appear (black color) in layover region yielding noisier image. The volume (Pv) and helix (Pc) scattering components are dominated at steep slope fore-slope area (N-W and S-W facing slope) and low values are found over snow covered area and back slope area (Fig. 1(c) and Fig. 1(d)).

Then the modified 4-CSPD method is applied to the same area to see the effect of the rotation (Fig.3). This method reduces the percentages of pixels with negative powers in Ps and Pd. Pixels with negative power in Ps and Pd are remained 7.7% and 9.8% respectively. It can be noticed after T_{33} rotation that the negative power occurrences are reduced 3.9% in Ps (Fig. 3(a)) and 19.7% in Pd (Fig. 3(b)) by modified method as compared to original method.

The decomposed power profiles are shown in Fig.4 (a)-(c), along a transect over the Satopanth glacier valley (see the transect in Fig. 4(a), 501 pixels profile on modified 4-CSPD False Color Composite (FCC) image in yellow color) for quantitative comparison of the original 4-CSPD method vs. the modified 4-CSPD method. The ablation area of glacier is highly crevassed and covered with moraine and debris material, which constitutes a very rough surface and creates multiple scattering, this cause shows high value of Pv in profile.

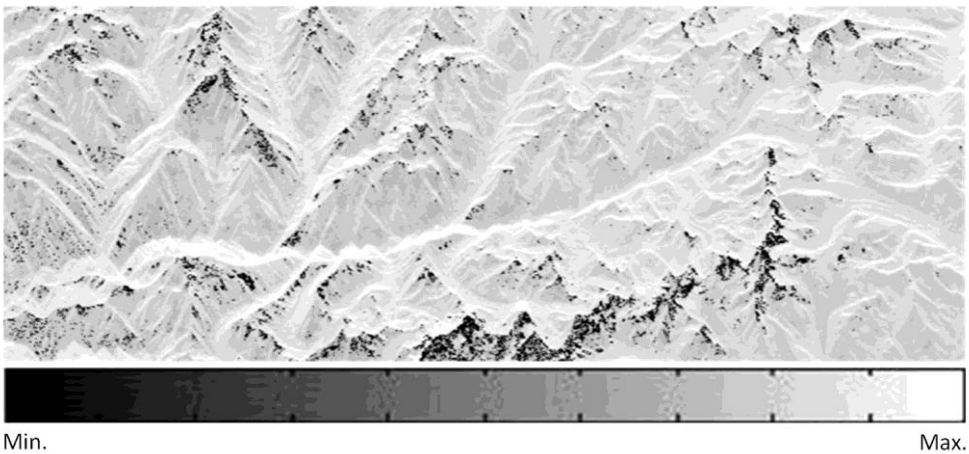

(a)

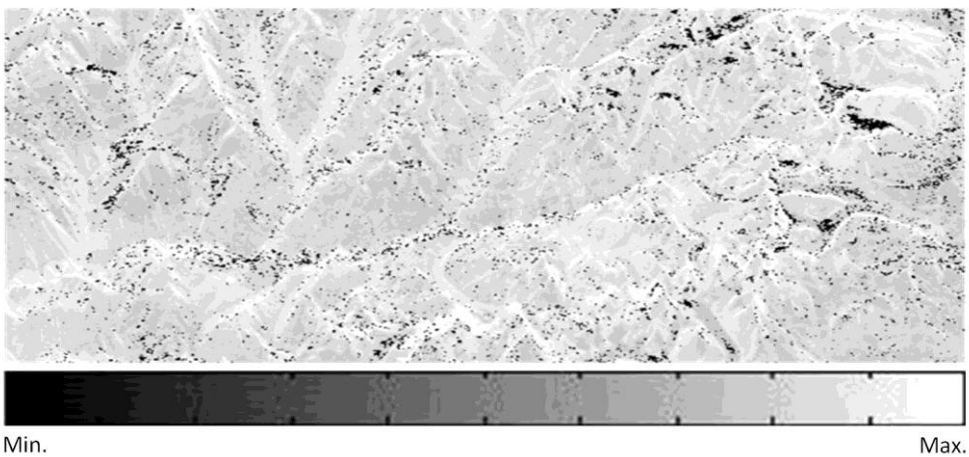

(b)

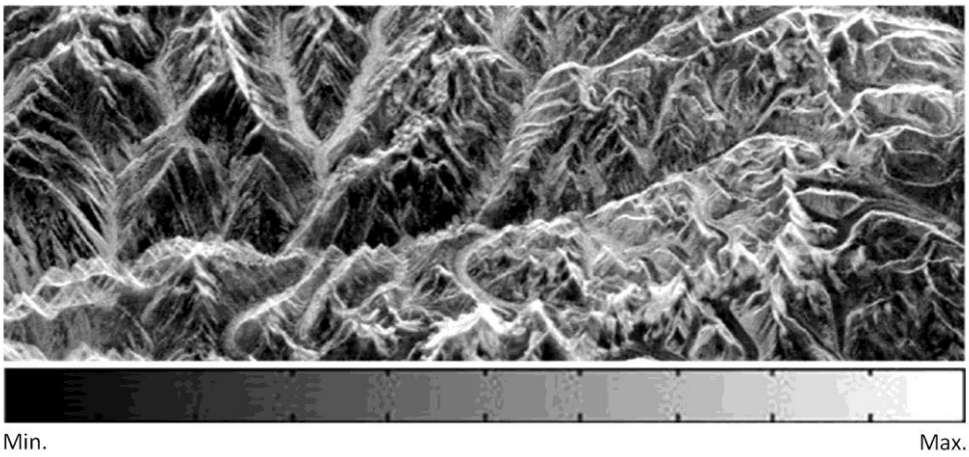

(c)

Fig. 3. 4-CSPD method decomposed powers with rotation of coherency matrix (a) Ps (b)Pd (c)Pv. Black areas in Ps image are 7.7% and in Pd image are 9.8% , which indicate the negative power occurred pixels.

In these profiles, less than -20dB value represents the negative power occurred pixels. Significant improvement in the negative power problem can be seen in Fig. 4 by the rotation of coherency matrix. Since Himalayan topography has gentle to steep slope, which behave like oriented target from the direction of radar that causes the over estimation volume scattering in original 4-CSPD method. But the modified 4-CSPD method compensates the orientation along the line of sight (LOS) while it decomposes the POLSAR data. The value of Pv is decreasing over the Satopanth glacier area, which is consistent with other experimental evidence (Yamaguchi *et. al*. 2011) avoiding over-estimation of the cross-polarized component. The values of Ps and Pd components increase after rotation. They are not fluctuating compared to the original case. Since the imaginary part T_{23} is roll-invariant (Lee and Ainsworth 2011) which is main source of the helix power Pc in 4-CSPD (Yamaguchi *et. al*. 2006, Yajima *et. al.* 2008). Therefore the value of Pc remains unchanged in modified 4-CSPD decomposition results. In addition, it can be seen that some of negative powers also appear after rotation (7.7% in Ps image and 9.8% in Pd image). These are inconsistent with the physical phenomena. Even though there

are significant improvements in reduction of negative powers, it is difficult to avoid all negative powers by new method (Yamaguchi *et. al*. 2011).The conditions of negative power occurrence in 4-CSPD are described in Yajima *et. al.* (2008).

Furthermore, technique of Yajima *et. al.* (2008) has been adopted to avoid remaining negative powers in decomposition results before making false color composite images. These RGB false color composite images with surface scattering (Blue), double bounce scattering (Red), and volume scattering (Green) are shown in Fig.5. In general, RGB false color composite images over Satopanth glacier region represent blue to deep blue color due to single scattering from snow cover over glacier area (accumulation zone) and permanent snow cover mountain peaks area. Red color represents double bounce or dihedral scattering mechanism. Debris covered glaciers (ablation area) correspond to green color area. Glacier moraines dam lakes are elucidated in deep blue color.

The differences are clearly seen between original and modified approach in Fig.6. Fig. 6 is an enlarged part of red color rectangular area in Fig. 5. Most of the change can be visibly identified in double bounce and surface scattering component of 4-CSPD method and these-components are clearly exposed in Fig. 6(b), with the help of rotated coherency matrix. It can be seen more “Blue” in (b) more than in (a). This indicates that the snow cover exhibiting “Blue” over the glacier area is enhanced by modified method as compared to original method.

The modified 4-CSPD method gives very sharp information about the double bounce features in the study area as compared to the original decomposition. The new application of this modified method will be useful to identify relatively permanent scatterer using time series data, which can be used for studying glacier movement.

Moreover, the quantitative analysis of decomposed power distribution is shown in Fig. 7 for 12 May 2007 data of PALSAR data within enlarged area. It is found that after rotation, Ps and Pd increase whereas Pv decreases.

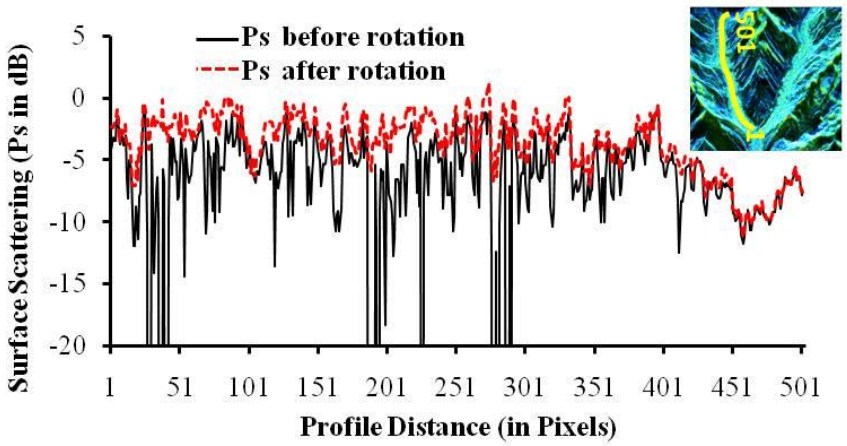

(a)

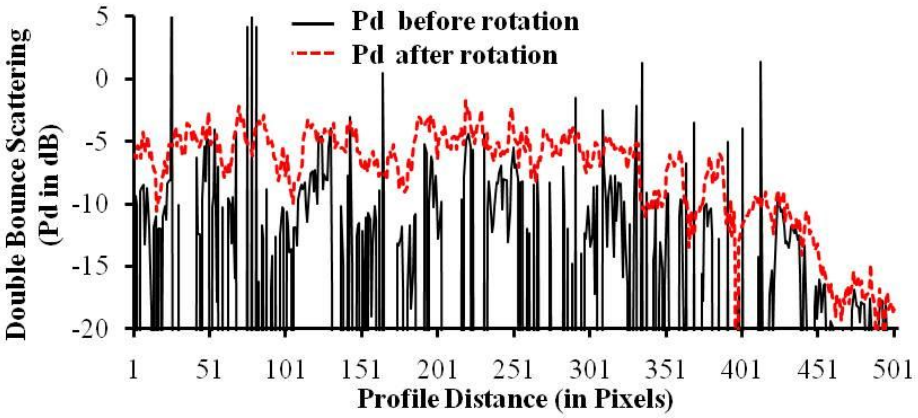

(b)

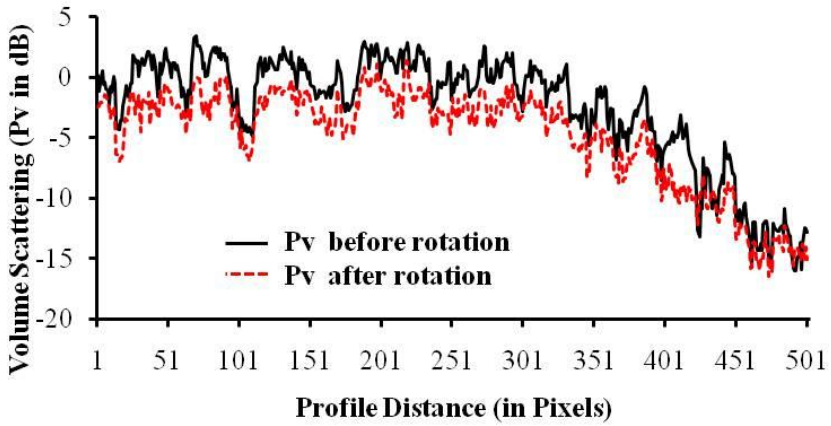

(c)

Fig.4. These profile show the original and modified 4-CSPD method scattering components over Satopanth Glacier (a) Ps (b)Pd and (c)Pv

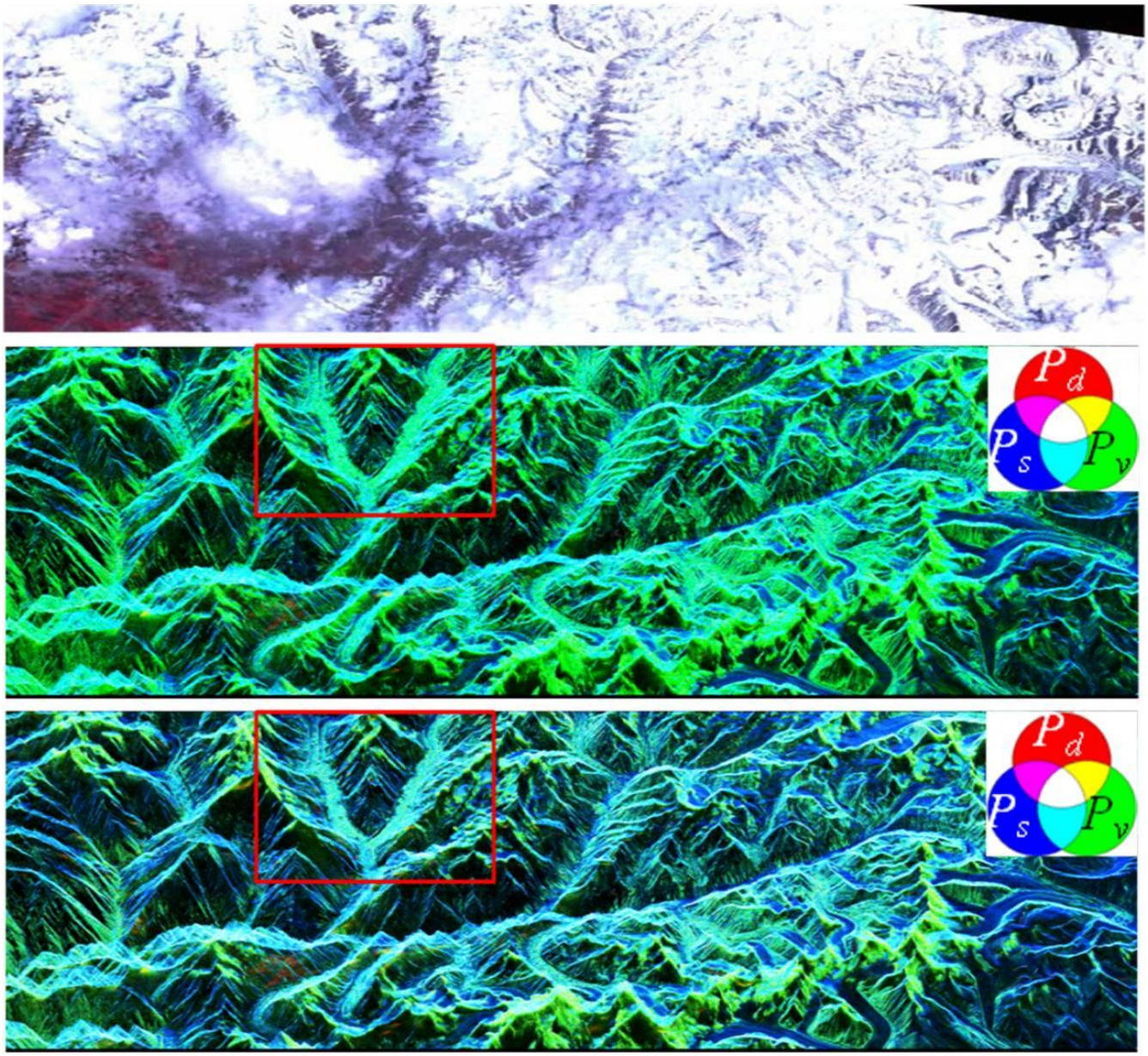

Fig. 5. ALOS-AVNIR-2 image of May 6, 2007 (upper), and 4-component scattering power decomposition (4-CSPD) false color composite (FCC) images with original coherency matrix of May 12, 2007 PALSAR data (middle) and with rotated coherency matrix of May 12, 2007 PALSAR data (bottom) (Red color rectangular on 4-CSPD method FCCs enlarged view are shown in Fig. 6).

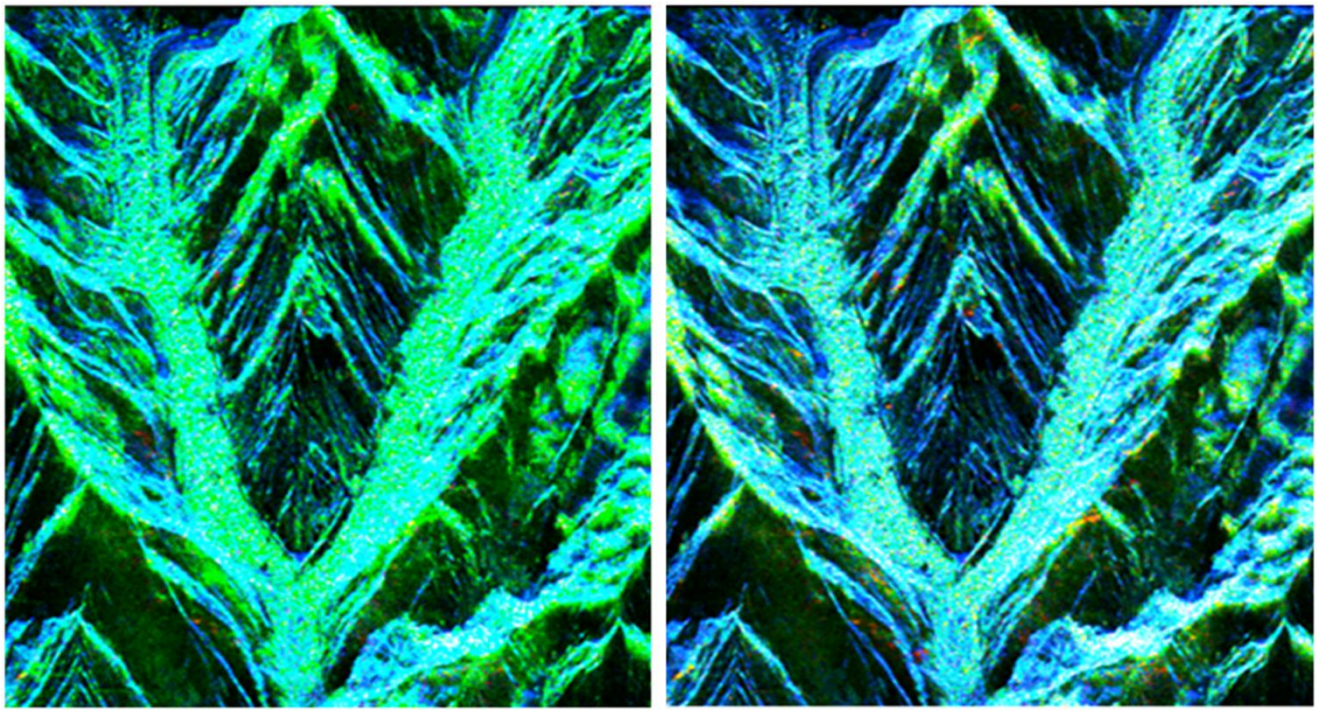

(a) (b)

Fig. 6. 4-component scattering power decomposition false color composite (Pd in “Red”, Pv in “Green” and Ps in “Blue”) images (a) with original coherency matrix of May 12, 2007 PALSAR data (b) with rotated coherency matrix of May 12, 2007 PALSAR data

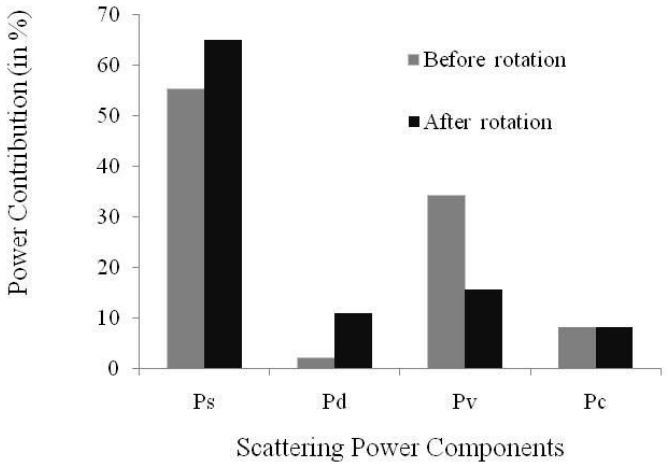

Fig. 7. 4-CSPD based power distribution before and after rotation of coherency matrix for red rectangular area (Fig.5) on 12 May 2007.

5. Conclusion

In this paper, fully polarimetric PALSAR data has been analyzed for high altitude glaciated terrain in Himalayan region based on modified 4-CSPD methods for extracting information from different type of terrain features. It has been found that the modified 4-CSPD method discriminates better terrain features like snow cover, dihedral (double bounce) and glacier features as compared to original 4-CSPD method. Since rotation angle become noisy at steep slope due to layover distortion in PALSAR image, a further modification 4-CSPD method based on rotation of coherency matrix cannot help too much for correctly discriminating targets in steep slope areas with single flight direction. In future work, both ascending and descending pass images will be used for correctly discriminating of targets in steep slope area by using presently discussed approach. Modification of 4-CSPD method will also be analyzed for detection of changes in glaciated terrain features during two temporal POLSAR images.

Acknowledgments

The authors would like to thank Japan Aerospace Exploration Agency for providing ALOS-PALSAR data sets under RA project. This work in part was carried out by Space Sensing Project, Ministry of Education, Japan.

References

Abe T., Yamaguchi Y. and Sengoku M., 1990. Experimental study of microwave transmission in snowpack, *IEEE Transactions on Geoscience and Remote Sensing*, 28 (5), 915-921.

Cloude, S.R. and Pottier, E., 1996. A review of target decomposition theorems in radar polarimetry. *IEEE Transactions on Geoscience and Remote Sensing*, 34, 498–518.

Dozier, J., 1989. Spectral signature of alpine snow cover from the Landsat Thematic Mapper, *Remote Sen. Environ.*, 28, 9-22, 1989

Freeman, A. and Durden, S.L., 1998. A three-component scattering model for polarimetric SAR data. *IEEE Transaction on Geoscience and Remote Sensing*, 36 (3), 936–973.

Gray, A. L. , *et. al.*, 1998. InSAR Results from the RADARSAT Antarctic Mapping Mission Data: Estimation of Glacier Motion using a Simple Registration Procedure, In: 1998 *International Geoscience and Remote Sensing Symposium*, 6-10 July, 1998, Seattle, Washington, New York: Institute of Electrical and Electronics Engineers (IEEE), 3, 1638 - 1640.

Lee, J. S. and Ainsworth, T., 2011 .The effect of orientation angle compensation on coherency matrix and polarimetric target decompositions, *IEEE Transaction on Geoscience and Remote Sensing*, 49(1), 53-64.

Lee, J. S., *et.al*., 2002. On the estimation of radar polarization orientation shifts induced by terrain slopes, *IEEE Trans. IEEE Transaction on Geoscience and Remote Sensing*, 40(1), 30-41.

Lee, J. S., Schuler, D.L., and Ainsworth, T.L., 2000. Polarimetric SAR data compensation for terrain azimuth slope variation, *IEEE Trans. IEEE Transaction on Geoscience and Remote Sensing*, 38(5), 2153-2163.

Lee, J.S. and Pottier, E. , 2009. *Polarimetric radar imaging from basic to applications*, Boca Raton: CRC Press, Taylor & Francis Group.

Michel, R. and Rignot, E., 1999. Flow of Glaciar Moreno, Argentina, from repeat-pass shuttle imaging radar images: comparison of the phase correlation method with radar Interferometry, *Journal of Glaciology*, 45(149), 93-100.

Mohite, K., *S*ingh, *G*., and Venkataraman, *G*., 2007. Feasibility of various remote sensing data for

mapping snow cover area around Gangotri Glacier, *Proc. of SPIE MIPPR*, 6787, (DOI:10.1117/12.753441)

Partington, K. C., 1998.Discrimination of glacier facies using multi-temporal SAR data, *Journal of Glaciology*, 44, 42-53.

Pottier, E., 1998. Unsupervised classification scheme and topography derivation of POLSAR data on the << H/A/α >> polarimetric decomposition theorem, *Proceedings of the Fourth International Workshop on Radar Polarimetry*, *13-17* July 1998,Nantes, France, Systemes Electroniques & Informatioues (SEI), 535 548.

Rott, H., 1994. Thematic studies in alpine areas by means of polarimetric SAR and optical imagery, *Advances in Space Research*, 14 (3), 217-226.

Shi, J., and Dozier, J., 2000. Estimation of Snow Water Equivalence Using SIR-C/X-SAR -Part I: Inferring Dry Snow Density and Subsurface Properties, *IEEE Transactions on Geoscience and Remote Sensing*, 38 (6), 2465–2474.

Shi, J., and Dozier, J., 1995. Inferring Snow Wetness Using C-band Data from SIR-C's Polarimetric Synthetic Aperture Radar, *IEEE Transactions on Geoscience and Remote Sensing*, 33 (4), 905-914.

Singh, G. and Venkataraman, G., 2009. LOS PALSAR data Analysis of snow cover area in Himalayan region using four component scattering decomposition model. *In: 2008 International conference of recent advances in microwave theory and applications* (*Microwave-08*), 21–24 November 2008, Jaipur, India. New York: Institute of Electrical and Electronics Engineers (IEEE), 772–774.

Singh, G., 2010. *SAR polarimetry techniques for snow parameters estimation*. Ph.D. Thesis, Indian Institute of Technology Bombay, India.

Singh, G., *et. al.*, 2010. Glaciated terrain classification using modified four component scattering decomposition model, *IEICE Technical Report*, 110(250), 13-17.

Singh, G., Yamaguchi, Y., and Park, S. E., 2011a. Utilization of four-component scattering power

decomposition method for glaciated terrain classification, *Geocarto International*,26 (5),377-389.

Singh, G., Yamaguchi, Y., and Park, S. E., 2011b.4-component scattering decomposition with phase rotation of coherency, In: 2011 *International Geoscience and Remote Sensing Symposium*, 24-29 July, 2011, Vancouver, Canada, New York: Institute of Electrical and Electronics Engineers (IEEE).

Xu, F., and Jin, Y.Q., 2005.Deorientation theory of polarimetric scattering targets and application to terrain surface classification, *IEEE Transaction on Geoscience and Remote Sensing*, 43(10), 2351-2364.

Yajima, Y., *et al.*, 2008. POLSAR image analysis of wetlands using a modified four component scattering power decomposition. *IEEE Transaction on Geoscience and Remote Sensing*, 46 (6), 1667–1673.

Yamaguchi, Y., *et. al.*, 2011. Four-component scattering power decomposition with rotation of coherency matrix, *IEEE Transaction on Geoscience and Remote Sensing*, 49(6), 2251- 2258.

Yamaguchi, Y., Yajima, Y., and Yamada, H., 2006. A four-component decomposition of POLSAR images based on the coherency matrix. *IEEE Geoscience and Remote Sensing Letter*, 3 (3), 292–296.